Exploring anaerobic fluorescence in *Methanococcus maripaludis* with the fluorescence-activating and absorption-shifting tag (FAST)

A Thesis SUBMITTED TO THE FACULTY OF THE UNIVERSITY OF MINNESOTA

BY

Eric Hernandez

IN PARTIAL FULFILLMENT OF THE REQUIREMENTS FOR THE DEGREE OF

MASTER OF SCIENCE

Advisor
Kyle C. Costa

June 2022

Acknowledgements

Finishing this thesis seemed like a task that used to seem miles away and insurmountable all at once, but I had a fantastic group of people working alongside me the whole way that helped me cross the finish line. First, I would like to thank Dr. Kyle Costa who gave me the opportunity to work and learn in his lab. He been a great mentor both in and out of the lab, and I feel like I learn something with every conversation we have. His zeal for scientific discovery is admirable and aspirational. I have grown a great deal as a scientist and as a professional, and it would not have been possible without him.

I want to thank all the members of the Costa Lab (Farid Halim, Dallas Fonseca, Leslie Day, Emily Hanson, Madison Loppnow, Abby Schmitt, and Elisa Kelsey) for their continued support and for providing a great environment in the laboratory. I also thank the Bazurto and Fixen labs for their input and exchange of ideas.

I would like to thank my committee members Dr. Jannell Bazurto and Dr. Jeffrey (Jeff) Gralnick for taking the time to serve on my committee and providing positivity and encouragement through this process.

Thank you to the BioTechnology Institute and The Department of Plant and Microbiology at the University of Minnesota, and The Army Research Office for their financial support.

To my partner Lauren Payne, thank you for always being by my side these past two years and beyond. Your endless support and encouragement were beyond valuable, and I can’t imagine this journey without you.

Abstract

Live-cell fluorescence imaging in methanogenic archaea has been limited due to the strictly anoxic conditions required for growth and issues with autofluorescence associated with electron carriers in central metabolism. Here, we show that the fluorescence-activating and absorption-shifting tag (FAST) when complexed with the fluorogenic ligand 4-hydroxy-3-methylbenzylidene-rhodanine (HMBR) overcomes these issues and displays robust fluorescence in *Methanococcus maripaludis*. We also describe a mechanism to visualize cells under anoxic conditions using a fluorescence microscope. Derivatives of FAST were successfully applied for protein abundance analysis, subcellular localization, and determination of protein-protein interactions. FAST fusions to both formate dehydrogenase (Fdh) and F_{420}-reducing hydrogenase (Fru) displayed increased fluorescence in cells grown on formate containing medium, consistent with previous studies suggesting increased abundance of these proteins in the absence of H_2. Additionally, FAST fusions to both Fru and the ATPase associated with the archaellum (FlaI) showed membrane localization in single cells observed using anoxic fluorescence microscopy. Additionally, split reporter translationally fused to the alpha and beta subunits of Fdh reconstituted a functionally fluorescent molecule *in vivo* via bimolecular fluorescence complementation. Lastly, we demonstrate an example in which FAST is able to validate the localization of an uncharacterized protein and provide a framework for future multi-color imaging that would empower further studies going forward. Together, these observations demonstrate the utility of FAST as a tool for studying members of the methanogenic archaea. Portions of this thesis have been submitted for publication in The Journal of Bacteriology.

Table of Contents

Acknowledgements i
Abstract ii
Table of Contents iv
List of Figures v
List of Tables vi
Introduction 1
Introduction to Methanogens 1
Common Challenges in Studying Methanogenic Archaea 1
Development of FAST-based Imaging 3
State of Self-Labeling Protein Tags and the Advantages of FAST 4
Research Objectives 5
Results 8
Expression of FAST1 in *M. maripaludis.* 8
Anoxic microscopy with a microscope housed inside of an anoxic chamber. 9
Evaluation of FruA localization and abundance during growth with H_2 or formate. 10
Quantifying expression of *fdhAB* with splitFAST and BiFC 12
Use of tandem FAST2 (tdFAST2) to observe cellular localization of FlaI. 13
Discussion 14
Conclusions and Future Directions 17
Materials and Methods 19
Appendix 1: Multicolor Imaging in *M. maripalu*dis 27
Introduction 27
Results 27
Discussion 28
Conclusions and Future Directions 29
Figures and Tables 31
Bibliography 46

List of Figures

Figure 1 30
Figure 2 31
Figure 3 32
Figure 4 33
Figure 5 34
Figure 6 35
Figure 7 36
Figure 8 37
Figure 9 38

List of Tables

Table 1 39
Table 2 43

Introduction

Introduction to Methanogens

Methanogenic archaea (methanogens) are responsible for producing most of the methane on Earth and are model organisms for studying cellular processes in the Archaea. Several organisms such as *Methanococcus maripaludis*, *Methanosarcina* spp., and *Methanothermobacter* spp. have been used extensively in genetic or biochemical studies to understand the physiology and metabolism of methanogens (1-3). This group of organisms are particularly important to study for economic and environmental reasons. Methane makes up approximately 20% of global greenhouse emissions and is thought to have more than 25 times the global warming potency than that of CO_2, the next most abundant greenhouse gas (4). Their unique ability to produce methane as a byproduct of their metabolism makes them interesting from a commercial standpoint since methane is a potent chemical feedstock and is used in modern rocket engines as fuel. While many of these organisms are hydrogenotrophic and directly consume hydrogen gas to drive forward methanogenesis, they can oxidize substrates such as formate to rapidly produce hydrogen on their own (5). Hydrogen is an important component used in production of high value compounds such as such as petroleum or ammonia (6). This group of organisms are essential for gaining a better understanding of global warming, carbon cycling, and are potential sources of industrial/biotechnological innovation.

Common Challenges in Studying Methanogenic Archaea

Methanogens are a unique and interesting group for a variety of reasons; however, they can be particularly difficult organisms to study. One of the most immediate reasons that can make research a challenge is that they are primarily strict anaerobic organisms that grow in very low redox environments. As such, model methanogens like *Methanococcus maripaludis* require anaerobic culture conditions and reagents. Careful consideration must be taken when manipulating cell cultures. For example, flushing ambient oxygen out of instruments and cell-contact solutions such as syringes and antibiotics is a routine but essential task. Direct manipulation of open cultures or cells on agar plates must be done in anaerobic chambers that require careful monitoring and upkeep to maintain anoxic conditions. It is these types of considerations that can complicate otherwise straight-forward work and introduce additional considerations.

While there have been many strategies and molecular tools developed to facilitate research of anaerobes such as these, robust tools for direct cell visualization via fluorescence microscopy have been lacking. Fluorescence microscopy and fluorescent protein analysis in general has revolutionized microbiology since the cloning of the green fluorescent protein (GFP) (7). Fluorescent protein tags are very powerful tools which allow for protein quantification, analysis of protein-protein interactions, and spatiotemporal characterization of cellular proteins. First, most standard fluorescent protein tags require oxygen for fluorophore maturation. Molecular oxygen carries out a specific reaction in the immature protein which causes it to adopt the active and fluorescent conformation (8). Methanogens such as *M. mariplaudis* require strict anoxic conditions for growth and therefore fluorescent proteins such as GFP or yellow

fluorescent protein (YFP) will never fully mature and function properly. Fluorescent analysis of methanogens is further complicated by the background autofluorescence due to the presence of the oxidized electron carrier coenzyme F_{420} (excitation peak centered at 420 nm, emission peak centered at 480 nm (9)). Coenzyme F_{420} is also highly abundant across this group of organisms as it is involved in many key steps of the methanogenesis pathway (10, 11). To date, studies employing fluorescence microscopy on methanogens have been restricted to enumeration or identification of cells via fluorescence *in situ* hybridization (FISH) or visualization by F_{420}-based autofluorescence (12, 13). While these are particularly useful tools, they are limited in their ability to answer deeper questions in regard to an organism's physiology or genetic expression patterns. Alternative oxygen independent probes such as FMN binding fluorescent proteins (e.g., LOV-based fluorescent proteins) typically have weak fluorescence intensity and often exhibit emission around 450 nm, overlapping with excitation/emission spectra of F_{420} (14). Immunofluorescence strategies using antibody-reporter conjugates typically involve aerobic steps and/or permeabilization of cells using harsh detergents, which preclude live-cell imaging of anaerobes. Another consequence of aerobic preparation of methanogenic organisms is that it causes the rapid oxidation of coenzyme F_{420} which leads to increased autofluorescence. Furthermore, immunofluorescence approaches introduce the possibility of interference with cellular function or molecular dynamics due to their very large size. Conventional antibodies used in these types of techniques such as a mouse IGG1 can be over 150 kDa which makes them far from ideal for live cell imaging (15).

Development of FAST-based Imaging

Recently, an oxygen independent fluorescent protein reporter known as the fluorescence-activating and absorption-shifting tag (FAST) has been developed and adapted in select anaerobic organisms (16-18). FAST is an engineered variant of photoactive yellow protein with a molecular mass of 14 kDa (16). Like GFP, FAST can be translationally fused to the N- or C-terminus of a gene of interest. By itself, FAST does not exhibit fluorescence; however, upon the addition of a fluorogenic ligand (fluorogen), the two complex together to produce a fluorescent product. The underlying mechanism behind this spectral shift is the deprotonation of the fluorogen. When the fluorogen becomes deprotonated, it undergoes a red-shift which changes its spectral properties. The FAST protein binds to the fluorogen in order to stabilize its deprotonated state and produce fluorescence. Multiple fluorogens consisting of 4-hydroxybenzylidene rhodanine (HBR) derivatives exist with each having unique excitation and emission properties upon binding to FAST, and variants of FAST have been developed that specifically bind a subset of fluorogens allowing for two color live-cell imaging (19, 20). HBR derivatives are membrane permeable and bind reversibly and specifically to FAST (16).

State of Self-Labeling Protein Tags and the Advantages of FAST

SNAP-tags and HaloTags are popular fluorescent reporters that function similarly to FAST in that their fluorescence is based upon specific binding interactions between a protein tag and an exogenous ligand of interest (21, 22). Unlike FAST, SNAP and HaloTags rely upon covalent interactions with their respective ligands. This makes visualizing the same cells repeatedly more difficult as photobleaching becomes more of

an issue over time whereas the FAST interaction functions through non-covalent interactions and is fully reversible. The label can be washed off and replenished as needed. Additionally, in the domain of archaea, transcription and translation are coupled which can lead to measurable changes in cellular expression within the order of minutes (23). FAST-fluorogen complexes do not require any significant incubation as their substrate labeling rates are extremely high (Typical K_{on} = ~ 3 – 6 x 10^7 $M^{-1} \cdot s^{-1}$) and multiple orders of magnitude greater than most SNAP-tag complexes which is why the latter requires significant time to incubate (16, 24). This can lead to loss of information or unavoidable limitations in time-sensitive processes for live-cell imaging while FAST enables immediate imaging upon fluorogen addition.

There are several reasons FAST is a particularly attractive molecular tool for studying obligate anaerobes such as methanogens. Most importantly, fluorescence is oxygen independent, and membrane permeability of the ligand allows for live-cell imaging. FAST complexes are inherently bright and emit fluorescence across a wide spectrum, avoiding the limitations of reporters such as FMN binding proteins. FAST fluorescence is reversible and quantitative, allowing for direct measurement of relative protein abundance (16, 25). Additionally, splitFAST was recently developed to visualize protein-protein interactions through bimolecular fluorescence complementation (BiFC) (26). Finally, as a small, translationally fused tag, FAST can be used to observe protein localization in live cells.

Research Objectives

The primary objectives of this project are two-fold. First, we aim to develop a simplified method for efficient collection and analysis of fluorescent data in *M. maripaludis*. As mentioned previously, there are a myriad of challenges historically associated with studying an organism that requires strict anoxic growth, therefore a high degree of streamlining and intuitiveness become much more important. Secondly, we aim to validate this system against historic data sets to confirm repeatable results in the pursuits of relative protein quantification, protein-protein interaction, and protein localization. There exist multiple expression data sets both on the protein level as well as the transcript level to compare the reliability of our fluorescent tags in determining expression levels. There has also been extensive work done previously characterizing protein complexes and discrete localization patterns in this organism which will not only serve to test the accuracy of our work, but also the precision and potential limitations in the pursuit of resolving sub-cellular features on such a small organism (cell diameter is ~1 μm (27)).

In this study, we demonstrate successful use of the FAST toolkit in *M. maripaludis,* demonstrating a functional fluorescence-based system for microscopic imaging in a methanogen. We developed a platform for microscopy under anoxic conditions, allowing for visualization of live cells. Combining these advances, we observed robust and quantifiable fluorescence of differentially expressed proteins in cells grown with either H_2 or formate as an electron donor, BiFC using the multisubunit formate dehydrogenase (Fdh), and two different examples of protein localization. This was accomplished using the original FAST protein, also referred to as FAST1, as well as a highly fluorescent, tandem variant. FAST-based fluorescence microscopy expands existing tools for studying the cell biology of *M. maripaludis* and should be broadly

applicable to other methanogens with established protocols for heterologous protein expression.

Results

Expression of FAST1 in *M. maripaludis*.

To test the functionality of FAST, a codon optimized FAST1 gene (Table 2) (28) was expressed in *M. maripaludis* on the replicating vector pLW40 under control of the *Methanococcus voltae* histone promoter (29). Under these conditions, heterologously expressed protein can reach up to 1% of total cellular protein (30). 4-hydroxy-3-methylbenzylidene-rhodanine (HMBR), a FAST fluorogen, was added to stationary phase cultures (OD_{600} = ~0.9) to a final concentration of 10 μM (based on manufacturer's recommendation) before transfer to a 96 well dark plate for quantification on a microplate reader. HMBR fluorescence was measured at 540 nm (excitation with 481 nm). Cultures that were not treated with HMBR exhibited little autofluorescence while cells containing both FAST1 and HMBR exhibited a significant increase in fluorescence (Fig. 1A). Addition of HMBR to wild type cells did not lead to a significant increase in fluorescence compared to cultures expressing FAST1 without HMBR addition.

To further optimize FAST1, we assessed autofluorescence of wild type cells during different stages of growth. We found that cells exhibited the lowest levels of autofluorescence prior to reaching OD_{600} = ~0.40 or ~1.0 in medium supplemented with formate or H_2 as the electron donor for growth, respectively (Fig. 7). We hypothesize that increased autofluorescence at higher OD_{600} is due to an accumulation of oxidized F_{420} when electron donors become growth limiting (31). We also noted that autofluorescence

was generally higher in cultures grown on H_2 and lower in cultures grown on formate; therefore, formate grown cells were used in subsequent experiments when possible. Additionally, we tested whether altering concentrations of HMBR could further optimize fluorescence over background. In general, increasing concentrations of HMBR led to increased fluorescence (Fig. 1B).

HMBR is generally regarded as non-toxic. To verify this is true for *M. maripaludis*, we assessed growth after exposing cells to HMBR. *M. maripaludis* expressing FAST1 on the plasmid pLW40 was grown in liquid overnight and then aliquots were prepared anaerobically in a chamber by adding HMBR to a final concentration of 20 μM, the highest concentration used in this study. After a 30-minute incubation, these cells were transferred to sterile medium and assessed for growth. There was no apparent difference in lag period or growth rate compared to controls that were not exposed to HMBR (Fig. 8). For all subsequent experiments, a concentration of 10 μM HMBR was used per manufacturer's recommendation, unless otherwise indicated.

Anoxic microscopy with a microscope housed inside of an anoxic chamber

Due to the oxygen sensitivity of *M. maripaludis*, live-cell imaging requires strict anoxia. To overcome this limitation, we developed a platform to perform fluorescence microscopy using an ECHO Revolve R4 hybrid microscope inside of a Coy anaerobic chamber (Fig. 2A). The microscope utilizes a computer tablet camera in place of an eyepiece, and all manipulations can be performed using a touch screen with a capacitive stylus. Using this system, HMBR addition, culture mounting, and imaging can all be performed without introducing oxygen. The microscope was operated in the upright orientation for all experiments.

Wild type *M. maripaludis* and the strain expressing FAST1 were examined both with and without fluorogen treatment (Fig. 2B). Only FAST1 expressing cells showed noticeable fluorescence gain upon HMBR addition. Because preparing samples in the anoxic chamber involves transferring cells from the high H_2 (or formate) concentrations of a culture tube to the low hydrogen atmosphere of the chamber (3%), cells were imaged immediately after preparation to mitigate the possibility of increasing autofluorescence from F_{420} oxidation.

Evaluation of FruA localization and abundance during growth with H_2 or formate

The F_{420}-reducing hydrogenase (Fru) catalyzes the reversible reduction of coenzyme F_{420} to $F_{420}H_2$ using H_2 as an electron donor and is the primary source of $F_{420}H_2$ for methanogenesis (32, 33). The large subunit of the hydrogenase, FruA, was selected as a test case for analyzing a FAST1 translational fusion. Fru is abundant in the cell, shows differential expression with increased abundance when formate is supplied as an electron donor for growth, and is thought to associate with the cell membrane (33-35). Using allelic replacement mutagenesis (1), two strains were created with FAST1 translationally fused to either the N terminus or C terminus of FruA. Both strains were analyzed during early exponential growth with either H_2 or formate as the electron donor.

The FAST1-FruA construct displayed a pattern of fluorescence consistent with the known membrane localization of Fru (33); however, this differed significantly from the pattern observed for the FruA-FAST1 fusion construct (Fig. 3A). Fluorescence in the C-terminal fusion was uniform across the cell while the N-terminal fusion exhibited distinctly higher fluorescence along the outer perimeter of the cell. The different

fluorescence pattern observed between the two FruA constructs is likely due to proteolytic cleavage of the nascent peptide, which is required for maturation of [Ni-Fe] hydrogenases (36). During maturation, Fru is likely proteolytically cleaved at the C terminus, resulting in the loss of the FAST1 tag from FruA-FAST1 fusions and retention of the tag in FAST1-FruA fusions (Fig. 3B). This cleaved FruA-FAST1 expressing strain likely retains FAST1 in the cytoplasm, leading to uniform cellular fluorescence, while the mature, processed, and nonfluorescent hydrogenase localizes to the membrane.

The FAST1-FruA fusion strain was further analyzed for differences in protein abundance between cells grown in medium containing H_2 or formate. Several transcriptomic and proteomic studies have suggested that Fru is more abundant in cultures grown under conditions where H_2 concentrations limit growth or when formate is provided as the sole electron donor (37-40). The FAST1-FruA fusion strain was examined by anoxic fluorescence microscopy during early exponential growth (OD_{600} = 0.2 – 0.4). As before, cultures were processed in the absence of oxygen, treated with final concentrations of 10 μM fluorogen, and placed on a glass slide for immediate viewing. To control for autofluorescence, light intensity was measured on a per cell basis in the absence of fluorogen and mean intensities of cells after fluorogen addition were normalized to the autofluorescence baseline. Cells grown utilizing formate as the sole electron donor had 1.76-fold higher fluorescence when compared to cells grown with H_2 (Fig. 3C), consistent with increased levels of Fru protein when H_2 concentrations are low.

Quantifying expression of *fdhAB* with splitFAST and BiFC.

Fdh is a multisubunit protein that is essential for growth on formate (5, 40); therefore, we selected Fdh for further validation of FAST1 in measurements of protein

abundance. Additionally, as FAST1 is amenable to analysis using BiFC to study protein-protein interactions (26), we generated FdhAB fusion constructs containing split versions of the FAST1 protein. FAST1 can be expressed as two nonfunctional pieces, NFAST (composed of the N terminal 114 amino acids of FAST1) and CFAST (composed of the subsequent 10 amino acids). With splitFAST, two interacting proteins can be tagged with NFAST and CFAST, and, if they colocalize, the pieces will reconstitute in the cell to form a fully functioning protein and fluoresce upon HMBR addition. *M. maripaludis* contains two isoforms of Fdh (41). Fdh1 was selected for analysis because strains lacking *fdh1* are incapable of growth with formate (5, 40) and transcriptomic and proteomic studies suggest that, like Fru, Fdh1 is more abundant in cultures grown under conditions where H_2 concentrations limit growth or when formate is provided as the sole electron donor (37).

An *M. maripaludis* strain with translational fusions encoding FdhA-NFAST and FdhB-CFAST was generated by allelic replacement of the endogenous genes. We additionally generated control strains containing either FdhA1-NFAST and Mtd-CFAST (Mtd is the F_{420}-dependent methylenetetrahydromethanopterin dehydrogenase) or FdhB1-CFAST and Mtd-NFAST. Mtd was chosen as a negative control for these studies as Mtd and Fdh are not known to interact and the genes encoding these two proteins exhibit similar patterns of expression (37, 40). Strains containing FdhA1-NFAST and FdhB1-CFAST, FdhA1-NFAST and Mtd-CFAST, or Mtd-NFAST and FdhB1-CFAST were analyzed by anoxic fluorescence microscopy. Relative fluorescence was measured on a per cell basis. Average fluorescence intensity was significantly higher in the strain

containing FdhA1-NFAST and FdhB1-CFAST, and both control strains with Mtd fusion constructs displayed similar levels of background fluorescence (Fig. 4A and B).

To further validate the use of FAST to measure relative protein abundance across growth conditions, the FdhA1-NFAST and FdhB1-CFAST containing strain was analyzed for fluorescence differences between H_2 and formate grown cells. In cells grown with formate, fluorescence intensity was 2.87-fold higher, consistent with increased Fdh abundance when H_2 concentrations are low (38) (Fig. 4C).

Use of tandem FAST2 (tdFAST2) to observe cellular localization of FlaI

In an attempt to further validate FAST for protein localization, we targeted the archaellum (archaeal flagellum) which displays polar localization in intact cells (42). In *M. maripaludis* the major membrane associated components of the archaellum are the anchor (FlaJ) and its associated ATPase (FlaI). Initial attempts to visualize archaella using FAST1 translational fusions were unsuccessful, and we hypothesized that this was due to low fluorescence intensity. To address this, we incorporated a modified version of FAST that has a lower dissociation constant for the fluorogen (FAST2) as a tandem reporter (tdFAST2) (43). This alternative reporter has been shown to achieve higher fluorescence in both bacterial and eukaryotic cells (17, 43).

To test fluorescence, a codon optimized tdFAST2 was transformed into *M. maripaludis* under control of the *M. voltae* histone promoter on the replicating plasmid pLW40neo. FAST1, tdFAST2, and WT were grown to OD_{600} of 0.9, and fluorescence was analyzed using a microplate reader and black, flat bottom 96 well plates across several concentrations of HMBR (Fig. 1B). Strains expressing tdFAST2 displayed significant increases in fluorescence over cells expressing FAST1. When normalized to

OD_{600} and controlling for the inherent fluorescence background, microplate reader assays showed that cells expressing tdFAST2 exhibited a 1.9 - 2.1-fold increase fluorescence over FAST1 upon HMBR addition.

A strain was generated expressing FlaI translationally fused to tdFAST2. These cells were viewed by fluorescence microscopy in an anoxic chamber as previously described except that they were treated with 20 μM HMBR. Robust fluorescence was observed associated with the cell membrane and localized to a single focus, consistent with polar localization of archaella (Fig. 5).

Discussion

Several features of FAST proteins make them ideal for studies in anaerobic organisms. These include the minimal manipulation required to achieve robust fluorescence, a suite of fluorogens with excitation/emission maxima across the visible spectrum (19), and several variant proteins (e.g., FAST1, FAST2, tdFAST, splitFAST, etc…) to facilitate a variety of studies (20, 26, 43). The use of FAST to assess differential protein abundance across growth conditions, protein localization, and protein-protein interactions in live cells of *M. maripaludis* represents a significant advance over previous studies that were limited to using FISH or autofluorescence to assess methanogen abundance (12, 13).

FAST proteins function with a variety of fluorogenic ligands. For example, binding of the HBR derivative 4-hydroxy-3,5-dimethoxybenzylidene rhodanine (HBR-3,5DOM) shifts the properties of FAST1 such that ex/em wavelengths are 518/600 nm (44). While HBR-3,5DOM resulted in functional fluorescent protein in *M. maripaludis*, overall fluorescence was lower relative to that of HMBR (Fig. 9), and we generally

observed higher background fluorescence from the culture medium, so HBR-3,5DOM was not used further. Autofluorescence was also an issue with cultures grown on H_2 containing medium, which led us to collect samples using cells grown on formate, when possible. However, we note that increased autofluorescence in H_2 medium is not a significant impediment to data collection as we could still assess differences in relative expression across growth conditions (Figs. 3 and 4). Autofluorescence was likely due to H_2 limitation as H_2 diffusion is outpaced by cellular consumption at higher density; under H_2 limitation, levels of oxidized, fluorescent F_{420} significantly increase (31). Additionally, removal of cultures from a shaking incubator during sample preparation and transfer to the anoxic chamber can impact H_2 diffusion, requiring rapid sample preparation and processing. Autofluorescence was less of an issue in cultures grown with formate, likely because formate is soluble in aqueous medium so diffusion does not limit growth.

FAST could be further optimized for use in *M. maripaludis* with the use of protein variants. A previous study with FAST2 and tdFAST2 in mammalian cell culture showed that these variants could achieve 1.7-fold and 3.8-fold higher fluorescence, respectively, compared to the original FAST1 (43). We found a more modest increase for tdFAST2 in *M. maripaludis* of ~2-fold. FAST2 has identical quantum yield, a very similar molar absorption value, and a lower dissociation constant than FAST1 (43); therefore, it is likely increased fluorescence with tdFAST2 was a result of the tandem nature of the reporter. The performance of tdFAST2 in *M. maripaludis* was consistent with observations in *Eubacterium limosa* where a 1.5-fold increase in brightness was observed (17).

Expression of FAST proteins in *M. maripaludis* could be accomplished using a high expression vector or under control of native promoters on the genome. Generally, total fluorescence was lower when FAST was expressed from native promoters, and cellular fluorescence varied with the use of different promoters. As a result, expression analysis was carried out on single cells using a microscope. For each fused gene, differences in fluorescence were reflective of observed difference in mRNA and protein abundance in previous transcriptomic and proteomic studies (37). For Fru, previous studies found that proteins were ~1.7-fold more abundant when formate was provided as the sole electron donor for growth or when H_2 concentrations were growth limiting. The FAST-based fluorescence pattern observed here is consistent with these data; mean fluorescence intensities for Fru were 1.76-fold higher when formate was provided as an electron donor. For Fdh, previous studies suggested that these proteins were 2- to 3-fold more abundant when cultures were grown on formate (10), consistent with the 2.87-fold increase in fluorescence for formate grown cells observed here. Together, these data validate the use of FAST protein fusions to measure relative differences in gene expression and protein abundance.

Protein localization applications typically require high fluorescence signal to spatially resolve cellular features. While autofluorescence can complicate these analyses, we successfully visualized the subcellular localization of two proteins that were hypothesized to associate with the cell membrane. Archaella in *M. maripaludis* are associated with the cell pole and tagging FlaI with tdFAST2 resulted in a single discrete focus characteristic of the hypothesized localization pattern. Localization of Fru to the cell membrane was previously inferred from immunogold labeling of this protein in *M.*

voltae (34) and from biochemical studies where Fru activity was enriched in membrane fractions (35). Here we provide a third line of evidence for membrane association of Fru. It remains unclear whether membrane association is required for Fru activity *in vivo*.

Protein fluorescence can be used to characterize protein-protein interactions using dual reporter constructs via fluorescence resonance energy transfer or using a single reporter via BiFC. We used splitFAST to tag both subunits of Fdh and observed robust fluorescence above background through BiFC. While modest increases of fluorescence above background were also observed in control strains expressing either NFAST or CFAST fused to Mtd, fluorescence from NFAST and CFAST fused to FdhA and FdhB was significantly higher than either control experiment. High background in control strains was likely because Mtd is most abundant when cultures are grown with formate (37, 38), and BiFC can occur through transient interactions between abundant proteins.

Conclusions and Future Directions

We have demonstrated the utility of FAST for protein analysis in *M. maripaludis*. Combined with anoxic microscopy, FAST allows for live cell imaging, protein localization, determining protein-protein interactions, and expression analysis. These tools should be broadly applicable in other methanogenic archaea with established methods for heterologous protein expression and allelic replacement. Alternative fluorogens and FAST reporter proteins may further expand the utility of FAST in these organisms. The application of anoxic fluorescence reporters presented here expands the already robust toolkit for molecular biology studies in the methanogenic archaea.

With the work done in this project to validate the general capabilities of FAST in this organism, it is now poised to answer more specific questions around this and related

organisms. *M. maripaludis* has been identified to be naturally competent, a term that describes an organism with the ability to take in and incorporate DNA from the environment (45). While there has been extensive research in this field with regards to bacteria, very little research has been done on the mechanisms and machinery underlying competency in archaea. Characterization of the natural competency pathway in *M. maripaludis* is of great interest to this research group. Previous investigative approaches utilized broader gain or loss of function assays such as deletion or overexpression of genes suspected to be involved in competency. Utilization of fluorescence microscopy with FAST can help fill in knowledge as to how these proteins facilitate DNA uptake and incorporation.

For example, gene MMJJ_13020, was identified through transposon mutagenesis assays as being essential for competency in *M. maripaludis* (unpublished data). Interruption or deletion of this gene abolishes competency in *M. maripaludis*, while overexpression increases plasmid uptake Bioinformatic sequence prediction found the gene to contain a single transmembrane helix. In order to validate membrane localization, this gene was tagged with tdFAST2 and viewed under the anaerobic microscope where it displayed distinct localization in the membrane of the cell (Fig. 6). This observation lends itself to further assays such as combining DNA staining with FAST fluorescence for colocalization approaches to further characterize the gain and loss of function seen when this gene is overexpressed or deleted, respectively. For instance, if MMJJ_13020 is involved in the direct uptake of DNA, cells overexpressing MMJJ_13020 may exhibit an increase in overall DNA uptake. This would be observed as having a more frequent or more intense overlap of MMJJ_13020 fluorescence and labeled DNA compared to cells

expressing the gene using its native promoter. Another possible observation is the development of stronger MMJJ_13020 foci at the point of DNA contact. This foci development is a response seen in fluorescent fusions of ComEA, a conserved protein responsible for DNA uptake across the outer membrane in competent bacteria. The archaeal type IV-like pilus itself can also be tagged and visualized for potential time lapse experiments. Similar experimental setups have been used in *Vibrio cholerae* to achieve related goals (46). *V. cholerae* is another naturally competent prokaryote that uses type IV pili to secure DNA from the environment and incorporate it into the cytoplasm. This process was visualized by Ellison et al. using a fluorescent microscopy time lapse utilizing fluorescently labeled pilins and DNA (46). Translating such an approach with FAST-labeled machinery would be a strong first step. Historically, protein tags such as GFP have been deemed as large enough to perturb the export of pilins as well as their function (47), however FAST1 is roughly half the size of GFP and may be a promising solution to this problem. Additional routes of analysis can now be pursued in elucidating various pathways in this organism and methanogens at large.

Materials and Methods

Strains, medium, and growth conditions.

Strains in this study are listed in Table 1 in the supplemental material. *M. maripaludis* was grown on McCas medium at 37°C with agitation, except that sodium sulfide was replaced by ammonium sulfide for liquid medium (45, 48). For growth in liquid medium, cultures were grown in 5 ml volumes in Balch tubes. When H_2 was supplied as the electron donor for growth, Balch tubes were pressurized to 280 kPa with an 80% H_2, balance CO_2 gas mix. When formate was supplied as the sole electron donor

for growth, McCas-formate medium was used at 37°C without agitation (49) and Balch tubes were pressurized to 210 kPa with an 80% N_2, balance CO_2 gas mix. For growth on agar plates, 1.5% noble agar was used, and cultures were grown in an anaerobic incubation vessel pressurized to 140 kPa with an 80% H_2, balance CO_2 gas mix as described (45). When necessary, the following antibiotics were added to medium at the noted concentrations: neomycin (1 mg ml^{-1}), puromycin (2.5 µg ml^{-1}), or 6-azauracil (0.25 mg ml^{-1}).

To assess the toxicity of HMBR, *M. maripaludis* strains expressing FAST1 on pLW40 were grown overnight and 495 µL aliquots were transferred to microcentrifuge tubes in a Coy anaerobic chamber. 5 µl of ddH_2O, DMSO, or 3mM HMBR (dissolved in DMSO) were added, and cells were left to incubate at room temperature for 30 minutes. After incubation, cells were inoculated into McCas medium and growth was monitored by measuring optical density at 600 nm.

Plasmid construction and transformation of *Escherichia coli*

Plasmids and primers are listed in Table 1 in the supplemental material. To generate FAST constructs, a codon optimized version of the gene was synthesized by Integrated DNA technologies. The codon optimized sequences were determined using the JCat codon optimizer (28) with default parameters with *M. maripaludis* selected as the organism. To generate the tdFAST2 construct, it was necessary to alter the sequence of the gene to prevent loss of the tandem sequence through homologous recombination. To accomplish this, the N-terminal copy of FAST2 was codon optimized in JCat using *M. maripaludis* as the selected organism and the C-terminal copy was codon optimized in

JCat using *Methanocaldococcus jannaschii*. The nucleotide sequences of the FAST1 and tdFAST2 genes used in this study can be found in Table 2. To further prevent homologous recombination within the tdFAST2 sequence, the 21 base pairs that separate the N-terminal and C-terminal copies were manually edited to reduce similarity to the 33-base pair linker that was consistently used for tagged constructs. In this case, the second most prevalent codon was chosen as determined by the Kazusa database (50).

To generate in-frame FAST constructs, genomic regions flanking either the N terminus or the C terminus of the gene of interest were amplified by PCR using primers suitable for downstream assembly using Gibson assembly (40). Codon optimized FAST1 or tdFAST2 with an additional 33-base pair linker sequence encoding a linker peptide (16) was also amplified by PCR. PCR products were assembled into XbaI/NotI digested pCRuptneo (49). pCRuptneo contains features for propagation in *E. coli* (origin of replication and ampicillin resistance gene) and for selection (neomycin selection) and counterselection (uracil phosphoribosyltransferase) in methanogens. For expression on pLW40 (29), FAST1 or tdFAST2 were PCR amplified and placed into the vector by Gibson assembly at the NsiI and AscI restriction sites under control of the *M. voltae* histone promoter.

Gibson assembled constructs were transferred to *E. coli* DH5α by electroporation. *E. coli* transformants were selected on lysogeny broth agar medium containing ampicillin (50 μg ml^{-1}). Plasmids were extracted using the PureLink Quick Plasmid Miniprep kit (Invitrogen) before transfer to *M. maripaludis*. All constructs were sequence verified by Sanger sequencing at the University of Minnesota Genomics Center.

Transformation of *M. maripaludis*

All strains used in this study were generated in an *M. maripaludis* background lacking the gene for uracil phosphoribosyltransferase (Δ*upt* mutant) (45). DNA was introduced into *M. maripaludis* using either a natural transformation method or a polyethylene glycol (PEG) mediated transformation method (1, 51). For splitFAST constructs, compound, sequential transformations were performed using the integrative vector pCRuptneo. NFAST and CFAST sequences were assembled by amplifying a truncated portion of codon optimized FAST1 sequence. Each splitFAST strain was transformed once with either NFAST or CFAST, subjected to selection and counterselection to remove the integrated pCRuptneo vector, then transformed again to incorporate the second tag.

Cultures for natural transformation were grown in McCas medium using a 2% vol/vol inoculum and H_2 as the electron donor. After overnight (~18 h) growth to stationary phase (OD_{600}, ~1), cultures were moved into a room temperature Coy anaerobic chamber (3% H_2, 10% CO_2 atmosphere). Plasmid DNA that was preequilibrated for 1 hour in the anaerobic chamber was mixed with 0.5 ml fresh McCas medium and added to the culture using a syringe. The culture/plasmid mixture was pressurized to 280 kPa with an 80% H_2, balance CO_2 gas mix and incubated at 37°C with agitation for 4 hours. After outgrowth, 0.2 mLs of culture material was transferred to medium containing antibiotic (neomycin for pCRuptneo or puromycin for pLW40) to select for transformants. After growth on neomycin, integrative vectors were allowed to resolve by overnight growth without selection. Mutants were isolated by plating onto 6-azauracil containing McCas agar and resulting colonies were screened by PCR.

PEG-mediated transformations followed the protocol of (1, 49) with all steps performed under anoxic conditions. Briefly, cultures were grown to OD_{600} of ~0.7 before washing in transformation buffer (TB: 50 mM Tris, 350 mM sucrose, 380 mM NaCl, 1 mM $MgCl_2$, pH 7.5). Washed cells were resuspended in 0.375 ml of TB and ~5 µg of plasmid DNA was added before addition of 0.225 ml PEG solution (40% wt/vol PEG 8000 in TB). After a 1-hour incubation, cells were washed twice in McCas medium, pressurized to 280 kPa with an 80% H_2, balance CO_2 gas mix and incubated at 37°C with agitation for at least 4 hours. After outgrowth, cultures were treated the same as for the natural transformation method.

Fluorescence Quantification Using a SpectraMax M2e plate reader

HMBR was purchased from The Twinkle Factory (https://www.the-twinkle-factory.com/) and solubilized in DMSO to a concentration of 2 mM as a stock solution for all experiments. *M. maripaludis* cells were grown in McCas medium with H_2 to stationary phase (OD_{600} = ~0.9) before analysis. *M. maripaludis* liquid culture was directly aliquoted wells of a black, flat bottom 96 well plate (Bioassay systems #P96FL), with 10 µM of HMBR (unless otherwise indicated in the text) to a final volume of 200 µL. Cells were incubated with HMBR for 60 seconds per the manufacturer's instructions before readings. Fluorescence was measured in a SpectraMax M2e plate reader (Molecular Devices) and analyzed in SoftMax Pro 7 software. Excitation wavelength was set to 481 nm and emission wavelength was set to 540 nm utilizing auto emission cutoff settings. Each sample was normalized to the baseline reading of the same sample without

fluorogen addition to correct for autofluorescence. Samples were further normalized on a per cell basis using OD_{600} of the cells prior to plate preparation.

Samples prepared with HBR-3,5DOM utilized the same methodology as samples treated with HMBR with the addition of a wash step. To reduce the high levels of autofluorescence in the media, cells were pelleted aerobically via centrifugation at 15,500 x g for two minutes and resuspended to their original volume with sterile ddH_2O.

Microscopy

Imaging was performed in a Coy-type anaerobic chamber with an environment of 3% H_2, balance N_2. The chamber also contained a 20 cm x 20 cm tray with drierite desiccant to control humidity. All imaging was performed using an ECHO Revolve R4 hybrid microscope operated in the upright orientation with a high-resolution condenser (numerical aperture 0.85, working distance 7 mm). Images were taken with the high gain setting on and exposure settings were modified depending on the genetic construct. Cells were viewed using a 40x fluorite objective lens (NA 0.75 and 0.51 mm) or a 100x fluorite oil phase objective lens (NA 1.30 and 0.2 mm). Fluorescence imaging was carried out using standard FITC filter sets.

To minimize autofluorescence, culture tubes were kept in the incubator until they were ready for immediate imaging. Samples were prepared by aliquoting liquid culture into microcentrifuge tubes and subsequently adding HMBR in DMSO to final concentrations as specified. Aliquots of 5 μL were added onto glass slides and glass coverslips were placed over them. All steps were performed under anoxic conditions.

Quantification of Fluorescence Microscopy Data using ImageJ

For expression analysis, 16-bit .tiff images of both a phase contrast and a fluorescent channel were used to analyze a single field of view utilizing a 40x objective. The FIJI package of ImageJ was used (version 2.1.0/1.53j Java ver. 1.8.0_172). A mask was generated using the phase contrast image by generating an 8-bit image using the threshold tool. The 'watershed' and 'fill holes' binary features were used as appropriate. The pixels of the resulting image in which cells were located were assigned a value of 1 and pixels elsewhere were assigned a value of 0 through the use of the division function. This image was multiplied with the corresponding fluorescence image to create a composite image with 32-bit float, and the mean fluorescence intensity per cell was determined using the particle analyzer feature. An average of averages was obtained from the compiled list of mean fluorescence intensities. Relative fluorescence units were determined by measuring the gain of fluorescence in cells after HMBR treatment. The average autofluorescent background was determined on a per-sample basis through the methods listed above and was subtracted from the values obtained after the addition of fluorogen. For protein localization analysis, 16-bit .tiff images of both a phase contrast and a fluorescence channel were used to analyze a single field of view utilizing a 100x objective. For figures, a median filter was applied for visual clarity and data are presented using the SuperPlotsOfData web application (52).

Statistical Analysis

Data are presented as means ± standard deviation. Statistical analysis was completed using a two tailed Student *t* test using Microsoft Excel software. P values for

Fdh splitFAST against negative controls were determined using a one-way ANOVA followed up by a post hoc Dunnett's test for multiple comparison significance in R (version 3.6.2) (53). Significant differences were considered when P values were < 0.05.

Data Availability

Images collected and analyzed in this study have been archived and are freely available at the Data Repository for the University of Minnesota (DRUM): https://hdl.handle.net/11299/227287

Acknowledgements

We thank Thomas Hanson for suggesting FAST as a potential reporter system and providing HMBR for preliminary experiments. This work was sponsored by a Young Investigator Program award from the Army Research Office, grant number W911NF-19-1-0024.

Appendix 1: Multicolor Imaging in *M. maripalu*dis

Introduction

Beyond tdFAST and FAST2, other variants of FAST have been developed and characterized for a variety of applications. Perhaps among the most attractive are greenFAST and redFAST. These two variants of FAST have had their specificity tuned for HMBR and HBR-3,5-DOM, respectively (20). Through protein engineering and screening facilitated by fluorescent-activated cell sorting (FACS), researchers introduced 3 amino acid mutations to the original FAST1 protein to reduce its affinity for HBR-3,5DOM by approximately two orders of magnitude and was named greenFAST for its enhanced specificity to HMBR (20). The redFAST reporter was created using the same methodology; 5 mutations were introduced that increased the dissociation constant for HMBR by two orders of magnitude and red-shifted the excitation maxima of the protein-ligand complex 40 nm (20). The excitation red-shift further serves to mitigate cross excitation between the HMBR + greenFAST complex and that of redFAST + HBR-3,5-DOM. As a result, orthogonality is achieved chemically and spectrally between these two reporters which resulted in a promising toolset for dual color FAST-based fluorescence investigations.

Results

We had attempted to utilize a codon optimized version of redFAST expressed on pLW40Neo to assess the feasibility of the redFAST-HBR-3, 5-DOM interaction in *M. maripaludis* (28). Initial plate reader analyses were carried out utilizing identical methods as those for tdFAST2 and FAST1 on pLW40 plasmids with the addition of a single wash

step utilizing ddH2O to remove the high autofluorescence of McCas media when utilizing these wave lengths. The resulting cell lysates showed no noticeable fluorescence after fluorogen treatment. This result was unexpected as redFAST shares a very high degree of similarity to FAST2 (95% identity on the amino acid level) which we have shown to perform well in *M. maripaludis* in the form of tdFAST2. In addition, we have already demonstrated that HBR-3, 5-DOM exhibits high fluorescence in *M. maripaludis* expressing tdFAST2 (Fig. 9). The sequences of these two differ by 6 amino acids which drew our attention to the codons of those 6 residues. Broad codon optimization is a widely used approach in recombinant protein expression, however there are times when the particular codon combinations chosen result in unexpected effects in translation initiation, translation efficiency, or they may negatively impact protein folding (54). The 5 differing residues were reasonable targets to begin troubleshooting. A new redFAST sequence was generated dubbed redFAST*. The new sequence was identical to the original codon optimized redFAST sequence apart from the 6 aforementioned amino acid residues which had their codons changed to the second most frequent codon in *M. maripaludis* using the Kazusa codon frequency database (55). WT *M. maripaludis* was transformed with pLW40Neo containing the revised redFAST sequence and still no apparent fluorescence was observed on preliminary plate reader assays.

Discussion

While HBR-3,5-DOM seems to work well when paired with cells expressing tdFAST2, no observable apparent fluorescence is visible when paired with redFAST. It remains uncertain why redFAST does not properly function in *M. maripaludis*. This is an unexpected outcome and complicates dual color visualization experiments that are useful

in co-expression or co-localization studies. The reasons for this may be specific to this organism as redFAST has been successfully utilized in another anaerobic organism recently. While this may complicate certain investigative approaches, it does not fully preclude FAST-based colocalization experiments or characterization of protein-protein interactions. As we have demonstrated with Fdh, splitFAST allows for robust detection of protein colocalization utilizing a single-color fluorescence approach.

Conclusions and Future Directions

Like redFAST, a FAST variant known as far red FAST (frFAST) has been developed to have high specificity for the HPAR-3OM fluorogen (56). The frFAST protein in conjunction with HPAR-3OM exhibit excitation and emission maxima at 555nm and 670nm, respectively which avoids overlapping spectra when used in conjunction with FAST1/FAST2-based reporters and HBR-3,5-DOM. While FAST1/FAST2 do not show noticeable interaction with HPAR-3OM, frFAST still shows observable binding to HBR-3,5-DOM which leads to uncertainty when determining sources of fluorescence in the case that both fluorogens are used for visualization (56). However, HBR-3,5-DOM has approximately 10 times greater affinity for FAST2 than frFAST (k_d = 0.41 uM and 3.9 uM, respectively (16).) This affinity gap coupled with the fact that the quantum yield of HBR-3,5-DOM + FAST2 is greater than twice that of HBR-3,5-DOM + frFAST help make them discrete reporters (16). Nonetheless, there exists a potential path forward for a system utilizing this combination of reporters and fluorogens especially if fluorogen concentrations are tuned appropriately.

While the use of redFAST remains restricted in M. maripaludis for the time being, there exist alternative fluorescent reporters that have had success in anaerobic conditions. Fortunately, the fluorescence-activating ligands for Halo-tags and SNAP-tags are orthogonal to the HMBR-derivatives that FAST interacts with (52). This leads to the possibility of discrete, multi-color labeling, however preliminary tests in this lab did not yield success with SNAP-tags in M. maripaludis. Halo-tags operate via a different chemistry and therefore may facilitate a path forward for multicolor imaging (21, 22). Such a system has been implemented in strictly anaerobic Clostridium organisms. Charubin et al. utilized SNAP-tags, Halo-tags, and FAST all at once to track population dynamics in mixed cultures (52). Ultimately, there are multiple routes to pursue for the purposes of multi-color fluorescence applications.

Figures

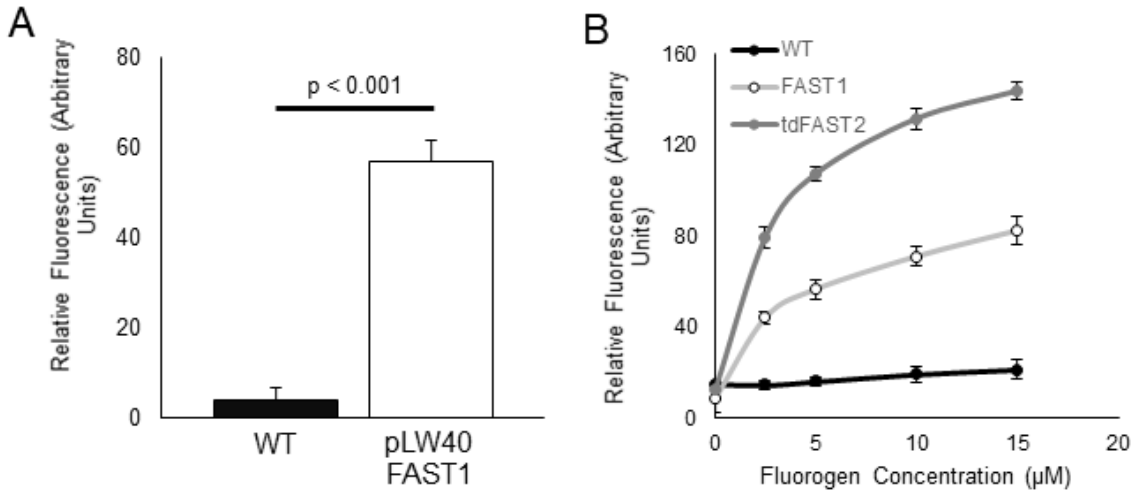

Figure 1

M. maripaludis expressing FAST is fluorescent upon HMBR addition **A.** Fluorescence intensities of *M. maripaludis* strains cultivated in McCas medium with H_2 as the electron donor for growth. HMBR was added to a final concentration of 10 μM. Relative fluorescence units were determined by normalizing emission readings from a microplate reader against baseline autofluorescence of the sample without fluorogen. Values were also normalized to the OD_{600} of the culture. **B.** Titration of HMBR in cells expressing FAST1 or the tandem variant tdFAST2 grown in McCas medium with H_2. Values were normalized to the OD_{600} of the culture. Data are averages and standard deviations of triplicate measurements.

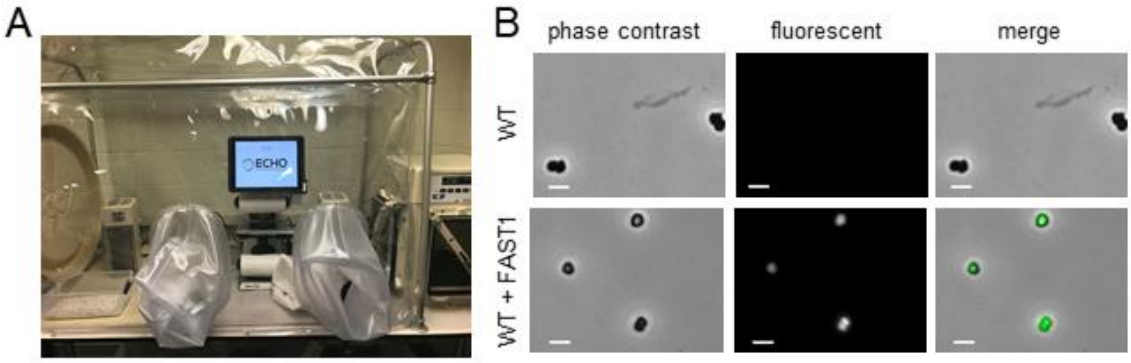

Figure 2

Anoxic microscopy of *M. maripaludis* expressing FAST1. **A.** The anoxic fluorescence microscope used in all experiments. **B.** Images of wild type *M. maripaludis* and a strain expressing FAST1 from the replicating vector pLW40. Scale bars = 2 μm.

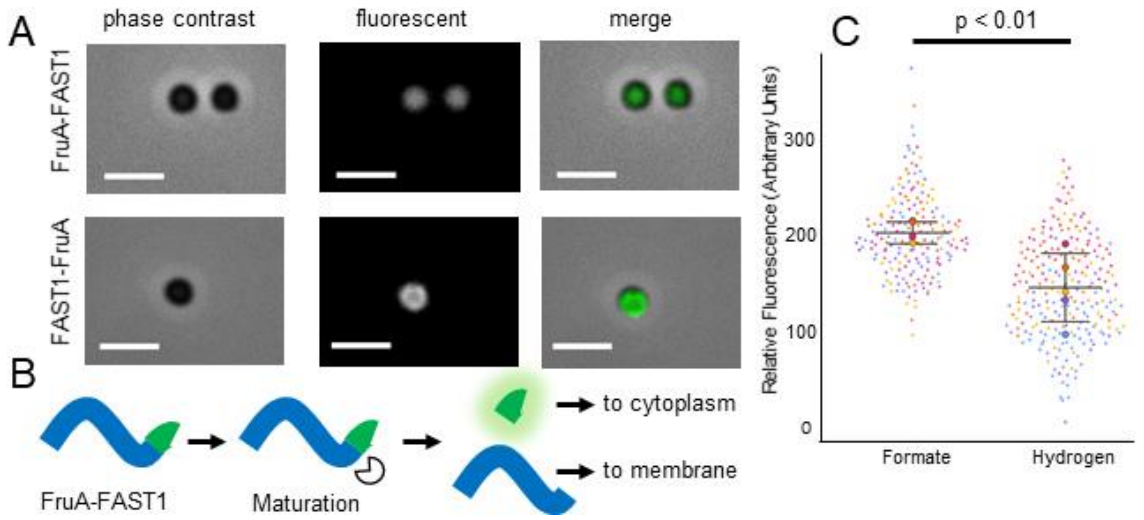

Figure 3

Cellular localization and expression N- and C-terminal translational fusions of FAST1 to FruA **A.** Images of N- and C-terminal FAST fusions to FruA. Scalebars = 2 μm. Arrows indicate locations of fluorescent foci associated with the cell membrane. **B.** Hypothesized maturation of the FruA peptide in the stain expressing *fruA*-FAST1. Maturation of FruA cleaves FAST from the mature hydrogenase. **C.** Fluorescence intensities of FAST1-FruA cells grown in medium with either formate (184 cells) or H_2 (236 cells) as the sole electron donor. Values were obtained by averaging fluorescence intensities of single cells from each sample via microscopy. Relative fluorescence was normalized to correct for autofluorescence in absence of fluorogen. Different circle colors represent data points from separate replicates, and mean values from all averaged cells in a replicate are represented by large circles. Data are averages and standard deviations from five independent cultures.

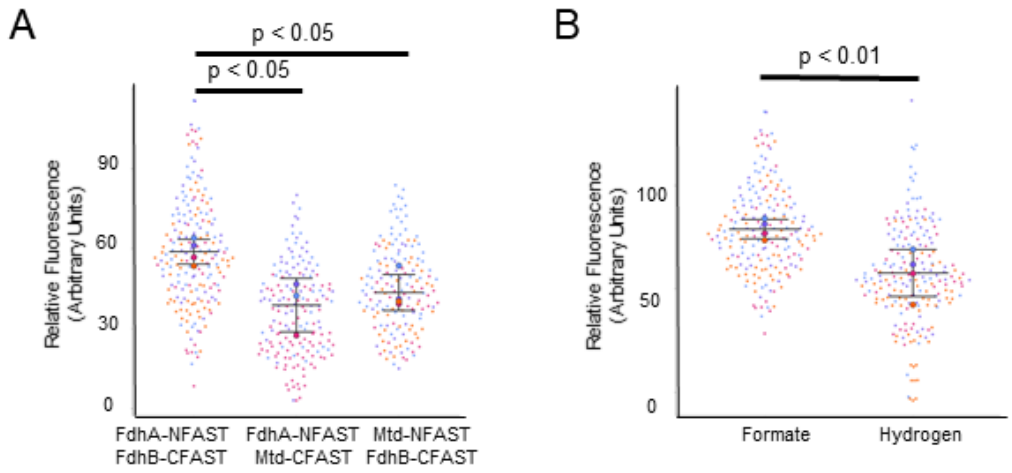

Figure 4

BiFC and fluorescence of Fdh1 with splitFAST **A.** Fluorescence intensities of cells grown expressing various splitFAST constructs. Negative controls *fdhA*-NFAST + *mtd*-CFAST (168 cells) and *mtd*-NFAST + *fdhB*-CFAST (160 cells) were compared to *fdhA*-NFAST + *fdhB*-CFAST (190 cells). Data were obtained using microscopy and are means and standard deviation of samples collected at least triplicate. **B.** Fluorescence intensities of *fdhA*-NFAST + *fdhB*-CFAST expressing cells grown in medium either formate (190 cells) or H_2 (183 cells) as the sole electron donor. Different circle colors represent data points from separate replicates, and mean values from all averaged cells in a replicate are represented by large circles. Data were obtained using microscopy and are means and standard deviation of quadruplicate samples.

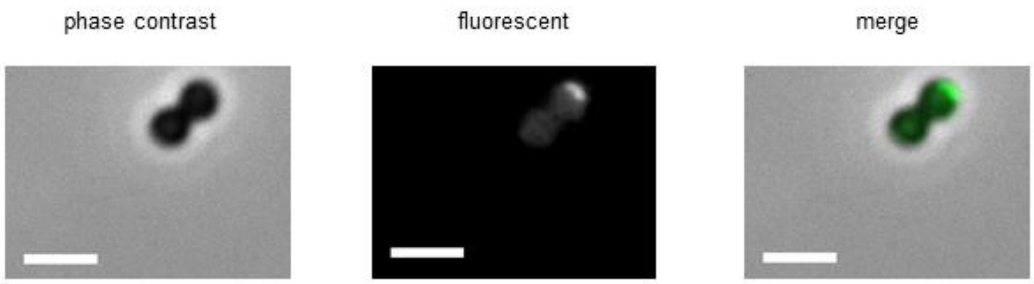

Figure 5

Localization of FlaI tagged with tdFAST2. Images are of early exponential phase cells treated with 20 μM HMBR. Scale bar = 2 μm.

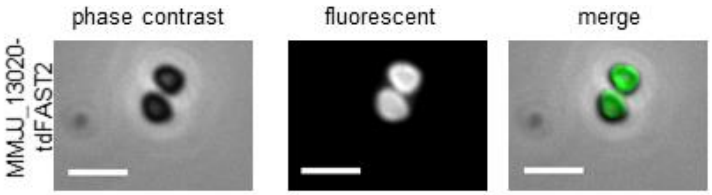

Figure 6

M. maripaludis expressing MMJJ_13020 tagged with tdFAST2. Cells are displaying highest fluorescent intensity around cell membrane suggesting membrane localization. Images are of hydrogen-grown cells treated with 20 μM HMBR. Scale bar = 2 μm.

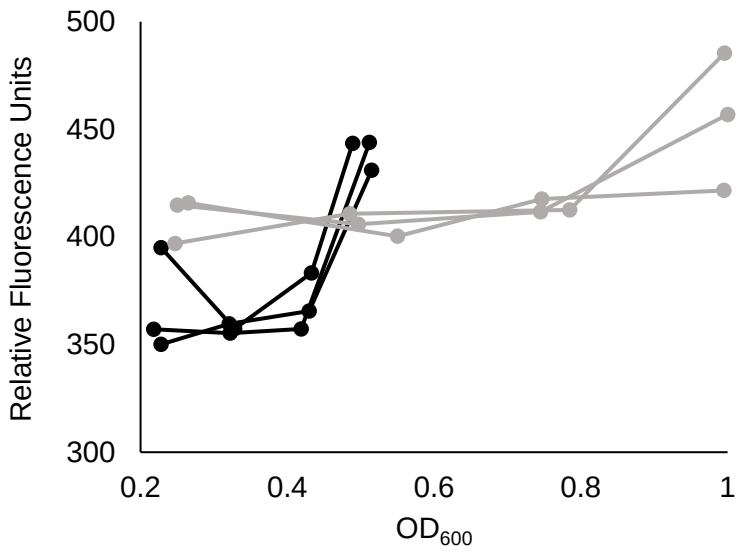

Figure 7

Autofluorescence of individual cells grown with either H_2 (grey lines) or formate (black lines) as the electron donor. Each line represents an independent culture. Formate grown cultures tend to reach stationary phase around an OD_{600} of 0.5 to 0.6, and H_2 grown cultures tend to reach stationary phase around an OD_{600} of 0.9 to 1.0.

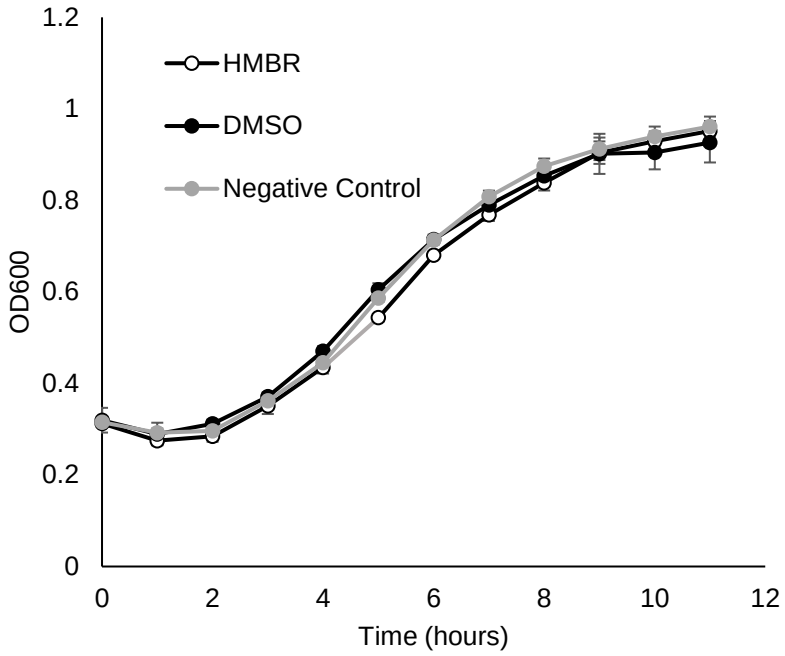

Figure 8

Growth of *M. maripaludis* expressing FAST1 after a 30-minute exposure to 20 µM HMBR. Data are averages and standard deviations of triplicate cultures.

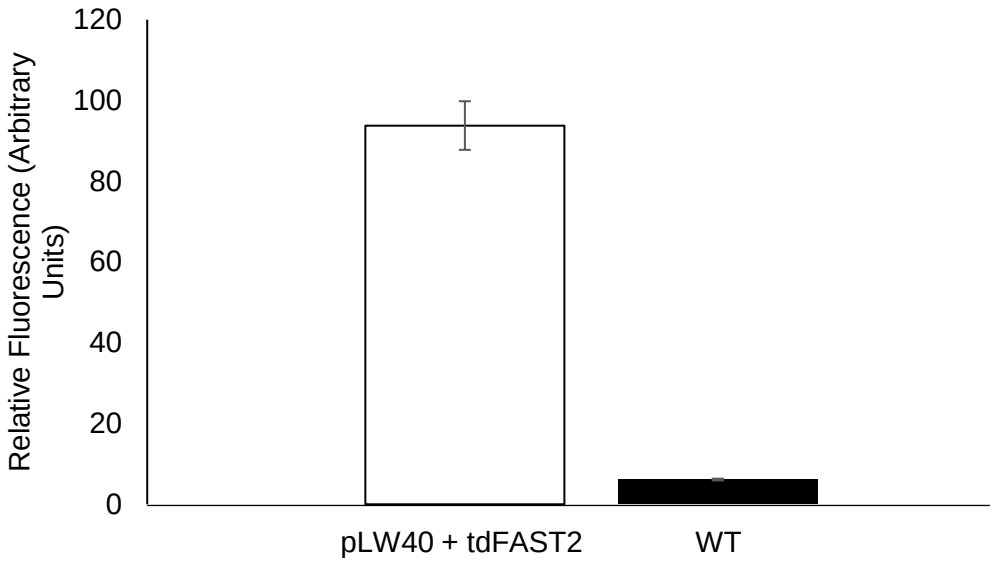

Figure 9

M. maripaludis expressing FAST is fluorescent upon HBR-3,5DOM addition. Fluorescence intensities of *M. maripaludis* strains cultivated in McCas medium with H_2 as the electron donor for growth. HBR-3,5DOM was added to a final concentration of 20 μM. Relative fluorescence units were determined by normalizing emission readings from a microplate reader against baseline autofluorescence of the sample without fluorogen. Values were also normalized to the OD_{600} of the culture. Data are averages and standard deviations of triplicate measurements.

Tables

Table 1

Strains, plasmids, and primers used in study

Strain	**Description**	**Reference**
KC13	*M. maripaludis* strain JJ ∆upt (MMJJ_RS02980)	Fonseca et al., 2020
KC90	KC13 expressing *FAST1* on pLW40neo	This study
KC91	KC13 expressing *fruA* tagged with FAST1 on the C-terminus	This study
KC92	KC13 expressing fruA tagged with FAST1 on the N-terminus	This study
KC93	KC13 expressing *fdh1A* tagged with NFAST at the C-terminus and *fdh1B* tagged with CFAST at the C-terminus	This study
KC94	KC13 expressing *fdh1A* tagged with NFAST at the C-terminus and *mtd* tagged with CFAST at the C-terminus	This study
KC95	KC13 expressing *mtd* tagged with NFAST at the C-terminus and *fdh1B* tagged with CFAST at the C-terminus	This study
KC96	KC13 expressing tdFAST2 on pLW40neo	This study
KC97	KC13 expressing *flaI* tagged with tdFAST2 on pLW40neo	This study
KC124	KC13 expressing MMJJ_13020 tagged with tdFAST2 at the C-terminus	This study
Plasmids		**Reference**
pCRuptneo	pCRprtneo plasmid containing the *upt* gene	Costa et al., 2010
pLW40	Replicative expression vector containing puromycin and ampicillin resistance genes	Dodsworth et al., 2006
pLW40neo	pLW40 with neomycin resistance cassettes	Dodsworth et al., 2006
	Sequence (5' - 3')	**Notes**
Primers used to generate KC90		
MM_co_YFAST-F-Nsi	AAAAATGCATGGAACACGTTGCATTCGG	NsiI
MM_co_YFAST_R-Asc	TTTTGGCGCGCCTTAAATCTTTTAACGAAAAC	AscI
Primers used to generate KC91		
Fru_YF_us_Fg	TGCAGATATCCATCACACTGGCGGCCGCATATTGCACAAACCGCAACAAACCAG	NotI
Fru-YF-us-Rg	CCGAATGCAACGTGTTCCATGAATTCTCTTATTTCAACAACTTTTTTAGTCTG	
YFAST_F	ATGGAACACGTTGCATTCGGATC	

YFAST_R	TTAAACTCTTTTAACGAAAACCCAG	
Fru_YF_ds_Fg	GTTTTCGTTAAAAGAGTTTAATAAATTCCTGAAAAGGAAAGTCTTG	
Fru_YF_ds_Rg	CTATAGGGCGAATTGGGCCCTCTAGAAACTTTAAAGTCTATTTCACGAG	XbaI
Primers used to generate KC92		
Fru_YF_N_us_Fg	TGCAGATATCCATCACACTGGCGGCCGCAAGGAACTATCGGAAGAAGCCTTGAAG	NotI
Fru_YF_N_us_Rg	CTGATCCGAATGCAACGTGTTCCATTTTATTCACCTCCAAGGGTAATATGC	
YFAST_Fr_N_Fg	ATGGAACACGTTGCATTCGGATCAG	
YFAST_Fr_N_Rg	TGATCCTCCTCCTCCTGATCCTCCTCCTCCTGAAACTCTTTTAACGAAAACCCAGTATG	
Fru-YF-N-ds-Fg	TCAGGAGGAGGAGGATCAGGAGGAGGAGGATCAGTGGCAGAACCTGTAACTATCAG	
Fru-YF-N-ds-Rg	CTATAGGGCGAATTGGGCCCTCTAGAGTGATGTTGGTTCTCATTCCACCAAC	XbaI
Primers used to generate KC93		
Fdh1B_CF_us_Fg	TGCAGATATCCATCACACTGGCGGCCGCCTGAAAAAGGTAAGCAGTTACTTG	NotI
Fdh1B_CF_us_Rg	CCTCCTGATCCTCCTCCTCCTGATTGAGTTGGGCATGACCCTCCAAG	
CFAST_10_F	TCAGGAGGAGGAGGATCAGGAGGAGGAGGATCAGGAGACTCATACTGGGTTTTCG	
Fdh1B_CFAST_10_R	CAGAACTAAAAAAATTAAAAAATAAATAATTAATAAATAATTTATTATCTTTTAACGAAAACCCAG	
Fdh1B_CF_ds_Fg	TAAATTATTTATTAATTATTTATTTTTTAATTTTTTTTAGTTCTG	XbaI
Fdh1B_CF_ds_Rg	TATAGGGCGAATTGGGCCCTCTAGAACATAATTCATGTTTTAGGATATGAAG	
Fdh1A_NF_us_Fg	TGCAGATATCCATCACACTGGCGGCCGCAAAGACTTGGTGTAGATGGACT	NotI
Fdh1A_NF_us_Rg	CTCCTCCTGATCCTCCTCCTCCTGATATTTTTTCCACCTTTGCAGCACATA	
NFAST_Fg	TCAGGAGGAGGAGGATCAGGAGGAGGAGGATCAATGGAACACGTTGCATTCGGATC	
NFAST_Rg	TGATAATGCTTTTTTCATGTG	
Fdh1A_NF_ds_Fg	CACATGAAAAAAGCATTATCATAATTTTCCCAAAATCGGGATTTTAAACGAG	
Fdh1A_NF_ds_Rg	TATAGGGCGAATTGGGCCCTCTAGAATCGATTTCTTCTTTTACAACG	XbaI
Primers used to generate KC94		

Fdh1A_NF_us_Fg	TGCAGATATCCATCACACTGGCGGCCGCAAAGACTTGGTGTAGATGGACT	NotI
Fdh1A_NF_us_Rg	CTCCTCCTGATCCTCCTCCTCCTGATATTTTTTCCACCTTTGCAGCACATA	
NFAST_Fg	TCAGGAGGAGGAGGATCAGGAGGAGGAGGATCAATGGAACACGTTGCATTCGGATC	
NFAST_Rg	TGATAATGCTTTTTTCATGTG	
Fdh1A_NF_ds_Fg	CACATGAAAAAAGCATTATCATAATTTTCCCAAAATCGGGATTTTAAACGAG	
Fdh1A_NF_ds_Rg	TATAGGGCGAATTGGGCCCTCTAGAATCGATTTCTTCTTTTACAACG	XbaI
Mtd_CF_us_Fg	TGCAGATATCCATCACACTGGCGGCCGCGATACGTTTTAATCAAATGCGAC	NotI
Mtd_CF_us_Rg	CTCCTGATCCTCCTCCTCCTGATTCTGGTTTTGTCATTAATTTACATTTG	
CFAST_10_F	TCAGGAGGAGGAGGATCAGGAGGAGGAGGATCAGGAGACTCATACTGGGTTTTCG	
Mtd_CFAST_10_R	GGTAAATTTTTTAATTTAAATGTAAATTTATTATCTTTTAACGAAAACCCAGTATGAG	
Mtd_CF_ds_Fg	TAAATTTACATTTAAATTAAAAAATTTACC	
Mtd_CF_ds_Rg	TATAGGGCGAATTGGGCCCTCTAGATTAATTGGAGTATGGTTTGCAATAG	XbaI
Primers used to generate KC95		
Mtd_NF_us_Fg	TGCAGATATCCATCACACTGGCGGCCGCGATACGTTTTAATCAAATGCGAC	
Mtd_NF_us_Rg	CTCCTGATCCTCCTCCTCCTGATTCTGGTTTTGTCATTAATTTAC	
NFAST_Fg	TCAGGAGGAGGAGGATCAGGAGGAGGAGGATCAATGGAACACGTTGCATTCGGATC	
NFAST_Rg	TGATAATGCTTTTTTCATGTG	
Mtd_NF_ds_Fg	CACATGAAAAAAGCATTATCATAAATTTACATTTAAATTAAAAAATTTACC	
Mtd-NF-ds-Rg	TATAGGGCGAATTGGGCCCTCTAGATTAATTGGAGTATGGTTTGCAATAG	
Fdh1A_NF_us_Fg	TGCAGATATCCATCACACTGGCGGCCGCAAAGACTTGGTGTAGATGGACT	NotI
Fdh1A_NF_us_Rg	CTCCTCCTGATCCTCCTCCTCCTGATATTTTTTCCACCTTTGCAGCACATA	
NFAST_Fg	TCAGGAGGAGGAGGATCAGGAGGAGGAGGATCAATGGAACACGTTGCATTCGGATC	
NFAST_Rg	TGATAATGCTTTTTTCATGTG	
Fdh1A_NF_ds_Fg	CACATGAAAAAAGCATTATCATAATTTTCCCAAAATCGGGATTTTAAACGAG	

Fdh1A_NF_ds_Rg	TATAGGGCGAATTGGGCCCTCTAGAATCGATTTCTTCTTTTACAACG	XbaI
Primers used to generate KC96		
Tdf2_plw40_mm_fg_2	GATAACTAATAGGTGAAATGCATGGAACACGTTGCATTCGGATCAGAAGACATC	AscI
Tdf2_plw40_mm_rg	CCTCCTCCTGATCCTCCTCCAACTCTTTTAACGAAAACCCAGTATGAGTCTCCTGATAAT	
Tdf2_plw40_mj_fg	GGAGGAGGATCAGGAGGAGGAGAACACGTTGCTTTTGGATCAGAAGATATTGAAAAT	
Tdf2_plw40_mj_rg	ACAGATCTCCTAGGCGCGCCTTAAACTCTTTTAACAAAAACC	NsiI
Primers used to Generate KC97		
FlaI-tdf2-us-Fg	TGCAGATATCCATCACACTGGCGGCCGCAAGGAGCTGTTGCTTTCCAGGCAATGC	NotI
FlaI-TDF2-us-Rg	CATAGATCCTCCTCCACCTGAACCTCCTCCTCCAGAAACCTGGAATGGCAGTCCTTCC	
tdf2-F	TCTGGAGGAGGAGGTTCAGGTGGAGGAGGATCTATGGAACACGTTGCATTCGGATCAGAAGACATC	
tdf2-R	TTAAACTCTTTTAACAAAAACCCAATATGAATCTCCTGATAAA	
FlaI-TDF2-ds-Fg	TTCATATTGGGTTTTTGTTAAAAGAGTTTAATAAGGTGTTTCTTATGTTTTTTGATATAC	
FlaI-YF-ds-Rg	CTATAGGGCGAATTGGGCCCTCTAGATTAATTCCTGACCGCTGTCTATTG	XbaI
PRIMERS USED TO GENERATE KC124		
PLW40_13020_PRIMER_1	GATAACTAATAGGTGAAATGCATGTCGTCTTTAATATTAAATGATAAAAAAATAAC	AscI
PLW40_13020_PRIMER_2	CATAGATCCTCCTCCACCTGAACCTCCTCCTCCAGAATCCCTTTCTTCACAGTAACTGC	
TDF2-F	TCTGGAGGAGGAGGTTCAGGTGGAGGAGGATCTATGGAACACGTTGCATTCGGATCAGAAGACATC	
PLW40_13020_PRIMER_4	ACAGATCTCCTAGGCGCGCCTTAAACTCTTTTAACAAAAACC	NsiI

Table 2

Nucleotide sequences of various FAST proteins used in this study

>FAST1
ATGGAACACGTTGCATTCGGATCAGAAGACATCGAAAACACATTAGCAAAAA
TGGACGACGGACAATTAGACGGATTAGCATTCGGAGCAATCCAATTAGACGG
AGACGGAAACATCTTACAATACAACGCAGCAGAAGGAGACATCACAGGAAG
AGACCCTAAACAAGTTATCGGAAAAAACTTCTTCAAAGACGTTGCACCTGGA
ACAGACTCACCTGAATTCTACGGAAAATTCAAAGAAGGAGTTGCATCAGGAA
ACTTAAACACAATGTTCGAATGGATGATCCCTACATCAAGAGGACCTACAAA
AGTTAAAGTTCACATGAAAAAAGCATTATCAGGAGACTCATACTGGGTTTTC
GTTAAAAGAGTTTAA

>tdFAST2
ATGGAACACGTTGCATTCGGATCAGAAGACATCGAAAACACATTAGCAAAAA
TGGACGACGGACAATTAGACGGATTAGCATTCGGAGCAATCCAATTAGACGG
AGACGGAAACATCTTACAATACAACGCAGCAGAAGGAGACATCACAGGAAG
AGACCCTAAACAAGTTATCGGAAAAAACTTCTTCAAAGACGTTGCACCTGGA
ACAGACTCACCTGAATTCTACGGAAAATTCAAAGAAGGAGTTGCATCAGGAA
ACTTAAACACAATGTTCGAATGGATGATCCCTACATCAAGAGGACCTACAAA
AGTTAAAATCCACATGAAAAAAGCATTATCAGGAGACTCATACTGGGTTTTC
GTTAAAAGAGTTGGAGGAGGATCAGGAGGAGGAGAACACGTTGCTTTTGGAT
CAGAAGATATTGAAAATACATTAGCTAAAATGGATGATGGACAATTAGATGG
ATTAGCTTTTGGAGCTATTCAATTAGATGGAGATGGAAATATTTTACAATATA
ATGCTGCTGAAGGAGATATTACAGGAAGAGATCCAAAACAAGTTATTGGAAA
AAATTTTTTTAAAGATGTTGCTCCAGGAACAGATTCACCAGAATTTTATGGAA
AATTTAAAGAAGGAGTTGCTTCAGGAAATTTAAATACAATGTTTGAATGGAT
GATTCCAACATCAAGAGGACCAACAAAAGTTAAAATTCACATGAAAAAAGCT
TTATCAGGAGATTCATATTGGGTTTTTGTTAAAAGAGTTTAA

>redFAST
ATGGAACACGTTGCATTCGGATCAGAAGACATCGAAAACACATTAGCAAAAA
TGGACGACGGACAATTAGACGGATTAGCATTAGGAGCAATCCAATTAGACGG
AGACGGAAACATCTTACAATACAACGCAGCACAAGGAGACATCACAGGAGC
AGACCCTAAACAAGTTATCGGAAAAAACTTCTTCAAAGACGTTGCACCTGGA
ACAGACTCACCTGAATTCTACGGAAAATTCAAAGTTGGAGTTGCATCAGGAA
ACTTAAACACAATGTTCGAATGGATGATCCCTACAAACAGAGGACCTACAAA
AGTTAAAGTTCACATGAAAAAAGCATTATCAGGAGACTCATACTGGGTTTTC
GTTAAAAGAGTTTAA

>redFAST*
ATGGAACACGTTGCATTCGGATCAGAAGACATCGAAAACACATTAGCAAAAA
TGGACGACGGACAATTAGACGGATTAGCATTGGGAGCAATCCAATTAGACGG
AGACGGAAACATCTTACAATACAACGCAGCACAGGGAGACATCACAGGAGC
TGACCCTAAACAAGTTATCGGAAAAAACTTCTTCAAAGACGTTGCACCTGGA
ACAGACTCACCTGAATTCTACGGAAAATTCAAAGTAGGAGTTGCATCAGGAA

ACTTAAACACAATGTTCGAATGGATGATCCCTACAAATAGAGGACCTACAAA
AGTTAAAGTTCACATGAAAAAAGCATTATCAGGAGACTCATACTGGGTTTTC
GTTAAAAGAGTTTAA

Bibliography

1. Sarmiento F, Leigh JA, Whitman WB. 2011. Genetic systems for hydrogenotrophic methanogens. Methods Enzymol 494:43-73.

2. Leigh JA, Albers SV, Atomi H, Allers T. 2011. Model organisms for genetics in the domain Archaea: methanogens, halophiles, *Thermococcales* and *Sulfolobales*. FEMS Microbiol Rev 35:577-608.

3. Thauer RK, Kaster AK, Seedorf H, Buckel W, Hedderich R. 2008. Methanogenic archaea: ecologically relevant differences in energy conservation. Nat Rev Microbiol 6:579-91.

4. Saunoise M. 2020. he Global Methane Budget 2000–2017, vol 12, p 1561-1623. Earth Syst. Sci. Data.

5. Lupa B, Hendrickson EL, Leigh JA, Whitman WB. 2008. Formate-dependent H2 production by the mesophilic methanogen *Methanococcus maripaludis*. Appl Environ Microbiol 74:6584-90.

6. Thomas G, Parks G. 2006. Potential Roles of Ammonia in a Hydrogen Economy. U.S. Department of Energy.

7. Chalfie M, Tu Y, Euskirchen G, Ward WW, Prasher DC. 1994. Green fluorescent protein as a marker for gene expression. Science 263:802-5.

8. Heim R, Prasher DC, Tsien RY. 1994. Wavelength mutations and posttranslational autoxidation of green fluorescent protein. Proc Natl Acad Sci U S A 91:12501-4.

9. Purwantini E, Mukhopadhyay B. 2009. Conversion of NO2 to NO by reduced coenzyme F420 protects mycobacteria from nitrosative damage. Proc Natl Acad Sci U S A 106:6333-8.

10. Wood GE, Haydock AK, Leigh JA. 2003. Function and regulation of the formate dehydrogenase genes of the methanogenic archaeon *Methanococcus maripaludis*. J Bacteriol 185:2548-54.

11. Deppenmeier U. 2002. The unique biochemistry of methanogenesis. Prog Nucleic Acid Res Mol Biol 71:223-83.

12. Kumar S, Dagar SS, Mohanty AK, Sirohi SK, Puniya M, Kuhad RC, Sangu KP, Griffith GW, Puniya AK. 2011. Enumeration of methanogens with a focus on fluorescence in situ hybridization. Naturwissenschaften 98:457-72.

13. Lambrecht J, Cichocki N, Hübschmann T, Koch C, Harms H, Müller S. 2017. Flow cytometric quantification, sorting and sequencing of methanogenic archaea based on F. Microb Cell Fact 16:180.

14. Buckley AM, Petersen J, Roe AJ, Douce GR, Christie JM. 2015. LOV-based reporters for fluorescence imaging. Curr Opin Chem Biol 27:39-45.

15. Vidarsson G, Dekkers G, Rispens T. 2014. IgG subclasses and allotypes: from structure to effector functions. Front Immunol 5:520.

16. Plamont MA, Billon-Denis E, Maurin S, Gauron C, Pimenta FM, Specht CG, Shi J, Quérard J, Pan B, Rossignol J, Moncoq K, Morellet N, Volovitch M, Lescop E, Chen Y, Triller A, Vriz S, Le Saux T, Jullien L, Gautier A. 2016. Small fluorescence-activating and absorption-shifting tag for tunable protein imaging in vivo. Proc Natl Acad Sci U S A 113:497-502.

17. Flaiz M, Ludwig G, Bengelsdorf FR, Dürre P. 2021. Production of the biocommodities butanol and acetone from methanol with fluorescent FAST-tagged proteins using metabolically engineered strains of *Eubacterium limosum*. Biotechnol Biofuels 14:117.

18. Streett HE, Kalis KM, Papoutsakis ET. 2019. A Strongly Fluorescing Anaerobic Reporter and Protein-Tagging System for. Appl Environ Microbiol 85.

19. Myasnyanko IN, Gavrikov AS, Zaitseva SO, Smirnov AY, Zaitseva ER, Sokolov AI, Malyshevskaya KK, Baleeva NS, Mishin AS, Baranov MS. 2021. Color Tuning of Fluorogens for FAST Fluorogen-Activating Protein. Chemistry 27:3986-3990.

20. Tebo AG, Moeyaert B, Thauvin M, Carlon-Andres I, Böken D, Volovitch M, Padilla-Parra S, Dedecker P, Vriz S, Gautier A. 2021. Orthogonal fluorescent chemogenetic reporters for multicolor imaging. Nat Chem Biol 17:30-38.

21. Keppler A, Gendreizig S, Gronemeyer T, Pick H, Vogel H, Johnsson K. 2003. A general method for the covalent labeling of fusion proteins with small molecules in vivo. Nat Biotechnol 21:86-9.

22. Los GV. 2005. HaloTag™ interchangeable labeling technology for cell imaging, protein capture and immobilization, vol 11, p 2-6. Promega Cell Notes.

23. Weixlbaumer A, Grünberger F, Werner F, Grohmann D. 2021. Coupling of Transcription and Translation in Archaea: Cues From the Bacterial World. Front Microbiol 12:661827.

24. Wilhelm J, Kühn S, Tarnawski M, Gotthard G, Tünnermann J, Tänzer T, Karpenko J, Mertes N, Xue L, Uhrig U, Reinstein J, Hiblot J, Johnsson K. 2021.

Kinetic and Structural Characterization of the Self-Labeling Protein Tags HaloTag7, SNAP-tag, and CLIP-tag. Biochemistry 60:2560-2575.

25. Monmeyran A, Thomen P, Jonquière H, Sureau F, Li C, Plamont MA, Douarche C, Casella JF, Gautier A, Henry N. 2018. The inducible chemical-genetic fluorescent marker FAST outperforms classical fluorescent proteins in the quantitative reporting of bacterial biofilm dynamics. Sci Rep 8:10336.

26. Tebo AG, Gautier A. 2019. A split fluorescent reporter with rapid and reversible complementation. Nat Commun 10:2822.

27. Goyal N, Zhou Z, Karimi IA. 2016. Metabolic processes *of Methanococcus maripaludis* and potential applications. Microb Cell Fact 15:107.

28. Grote A, Hiller K, Scheer M, Münch R, Nörtemann B, Hempel DC, Jahn D. 2005. JCat: a novel tool to adapt codon usage of a target gene to its potential expression host. Nucleic Acids Res 33:W526-31.

29. Dodsworth JA, Leigh JA. 2006. Regulation of nitrogenase by 2-oxoglutarate-reversible, direct binding of a PII-like nitrogen sensor protein to dinitrogenase. Proc Natl Acad Sci U S A 103:9779-84.

30. Gardner WL, Whitman WB. 1999. Expression vectors for *Methanococcus maripaludis*: overexpression of acetohydroxyacid synthase and beta-galactosidase. Genetics 152:1439-47.

31. de Poorter LMI, Geerts WJ, Keltjens JT. 2005. Hydrogen concentrations in methane-forming cells probed by the ratios of reduced and oxidized coenzyme F420. Microbiology (Reading) 151:1697-1705.

32. Hendrickson EL, Leigh JA. 2008. Roles of coenzyme F420-reducing hydrogenases and hydrogen- and F420-dependent methylenetetrahydromethanopterin dehydrogenases in reduction of F420 and production of hydrogen during methanogenesis. J Bacteriol 190:4818-21.

33. Baron SF, Ferry JG. 1989. Purification and properties of the membrane-associated coenzyme F420-reducing hydrogenase from *Methanobacterium formicicum*. J Bacteriol 171:3846-53.

34. Muth E. 1988. Localization of the F 420 -reducing hydrogenase in *Methanococcus voltae* cells by immuno-gold technique, vol 150, p 205-207, Archives of Microbiology.

35. Baron SF, Williams DS, May HD, Patel PS, Aldrich HC, Ferry JG. 1989. Immunogold localization of coenzyme F 420 -reducing formate dehydrogenase

and coenzyme F 420 -reducing hydrogenase in *Methanobacterium formicicum*, vol 151, p 307-313. Archives of Microbiology.

36. Lacasse MJ, Zamble DB. 2016. [NiFe]-Hydrogenase Maturation. Biochemistry 55:1689-701.

37. Costa KC, Yoon SH, Pan M, Burn JA, Baliga NS, Leigh JA. 2013. Effects of H2 and formate on growth yield and regulation of methanogenesis in *Methanococcus maripaludis*. J Bacteriol 195:1456-62.

38. Xia Q, Wang T, Hendrickson EL, Lie TJ, Hackett M, Leigh JA. 2009. Quantitative proteomics of nutrient limitation in the hydrogenotrophic methanogen *Methanococcus maripalu*dis. BMC Microbiol 9:149.

39. Hendrickson EL, Liu Y, Rosas-Sandoval G, Porat I, Söll D, Whitman WB, Leigh JA. 2008. Global responses of *Methanococcus maripaludis* to specific nutrient limitations and growth rate. J Bacteriol 190:2198-205.

40. Costa KC, Lie TJ, Xia Q, Leigh JA. 2013. VhuD facilitates electron flow from H2 or formate to heterodisulfide reductase in Methanococcus maripaludis. J Bacteriol 195:5160-5.

41. Poehlein A, Heym D, Quitzke V, Fersch J, Daniel R, Rother M. 2018. Complete Genome Sequence of the Methanococcus maripaludis Type Strain JJ (DSM 2067), a Model for Selenoprotein Synthesis in Archaea. Genome Announc 6.

42. Jarrell KF, Stark M, Nair DB, Chong JP. 2011. Flagella and pili are both necessary for efficient attachment of *Methanococcus maripaludis* to surfaces. FEMS Microbiol Lett 319:44-50.

43. Tebo AG, Pimenta FM, Zhang Y, Gautier A. 2018. Improved Chemical-Genetic Fluorescent Markers for Live Cell Microscopy. Biochemistry 57:5648-5653.

44. Li C, Plamont MA, Sladitschek HL, Rodrigues V, Aujard I, Neveu P, Le Saux T, Jullien L, Gautier A. 2017. Dynamic multicolor protein labeling in living cells. Chem Sci 8:5598-5605.

45. Fonseca DR, Halim MFA, Holten MP, Costa KC. 2020. Type IV-Like Pili Facilitate Transformation in Naturally Competent Archaea. J Bacteriol 202.

46. Ellison CK, Dalia TN, Vidal Ceballos A, Wang JC, Biais N, Brun YV, Dalia AB. 2018. Retraction of DNA-bound type IV competence pili initiates DNA uptake during natural transformation in *Vibrio cholerae*. Nat Microbiol 3:773-780.

47. Lagage V, Uphoff S. 2018. Filming flagella and pili in action. Nat Rev Microbiol 16:584.

48. Moore BC, Leigh JA. 2005. Markerless mutagenesis in *Methanococcus maripaludis* demonstrates roles for alanine dehydrogenase, alanine racemase, and alanine permease. J Bacteriol 187:972-9.

49. Costa KC, Wong PM, Wang T, Lie TJ, Dodsworth JA, Swanson I, Burn JA, Hackett M, Leigh JA. 2010. Protein complexing in a methanogen suggests electron bifurcation and electron delivery from formate to heterodisulfide reductase. Proc Natl Acad Sci U S A 107:11050-5.

50. Gibson DG, Young L, Chuang RY, Venter JC, Hutchison CA, Smith HO. 2009. Enzymatic assembly of DNA molecules up to several hundred kilobases. Nat Methods 6:343-5.

51. Tumbula DL, Makula RA, Whitman WB. 1994. Transformation of *Methanococcus maripaludis* and identification of a *Pst* I-like restriction system, vol 121, p 309-314. FEMS Microbiology Letters.

52. Charubin K, Streett H, Papoutsakis ET. 2020. Development of Strong Anaerobic Fluorescent Reporters for *Clostridium acetobutylicum* and *Clostridium ljungdahlii* Using HaloTag and SNAP-tag Proteins. Appl Environ Microbiol 86.

53. Team RCD. 2019. A language and environment for statistical computing, R Foundation for StatisticalComputing, Vienna, Austria.

54. Mauro VP, Chappell SA. 2018. Considerations in the Use of Codon Optimization for Recombinant Protein Expression. Methods Mol Biol 1850:275-288.

55. Nakamura Y, Gojobori T, Ikemura T. 2000. Codon usage tabulated from international DNA sequence databases: status for the year 2000. Nucleic Acids Res 28:292.

56. Li C, Tebo AG, Thauvin M, Plamont MA, Volovitch M, Morin X, Vriz S, Gautier A. 2020. A Far-Red Emitting Fluorescent Chemogenetic Reporter for In Vivo Molecular Imaging. Angew Chem Int Ed Engl 59:17917-17923.